Polymer Bulletin (2019) 76:3819–3839
https://doi.org/10.1007/s00289-018-2583-8

ORIGINAL PAPER

Preparation and properties evaluation of nitrile rubber nanocomposites reinforced with organo-clay, $CaCO_3$, and SiO_2 nanofillers

Mehran Sadeghalvaad[1] · Erfan Dabiri[2] · Sara Zahmatkesh[3] · Pooneh Afsharimoghadam[4]

Received: 27 June 2018 / Revised: 25 September 2018 / Accepted: 22 October 2018 /
Published online: 27 October 2018

Abstract

Acrylonitrile butadiene rubber (NBR)-based nanocomposites reinforced with organo-clay, calcium carbonate, and silica as nanofillers with different contents ranging from 1 to 10 phr (part per hundred parts of rubber) were prepared and characterized. Surface modification was done on the clay nanoparticles to intensify the formation of chemical bond between nanofiller and NBR matrix. A novel procedure and formula were implemented to fabricate considered composites and nanocomposites. Variety of tests and analyzes were done on all nanofillers and fabricated nanocomposites and accordingly, curing conditions, mechanical and chemical properties of the resulting NBR nanocomposites intercalated with nanofillers were further improved and optimized. The nanocomposite containing 10 phr of nanoorganoclay were found to be the best choice among other synthesized nanocomposites in the case of improved curing conditions, mechanical, and chemical properties.

Keywords Nitrile rubber · Nanocomposite · Nanomaterial · Mechanical properties

✉ Mehran Sadeghalvaad
m.sadeghalvaad@gmail.com

[1] Nano Chemical Engineering Department, Faculty of Advanced Technologies, Shiraz University, Shiraz, Iran

[2] Department of Gas Engineering, Ahwaz Faculty of Petroleum, Petroleum University of Technology, Ahwaz, Iran

[3] Department of Materials Science and Engineering, Faculty of Engineering, Shiraz University, Shiraz, Iran

[4] Department of Earth Sciences, College of Science, Shiraz University, Shiraz, Iran

Introduction

Adding fillers to polymer-based composites, as a method for improving their mechanical properties, thermal stability, and resistance against solvents has attracted many attentions among researchers. Filler materials are usually used for the purpose of improvement in a specific property or reduce the cost of composites synthesis [1, 2]. The improvement rate of properties by adding fillers to the polymer matrix is dependent on the filler/polymer base system and the specific surface area between them, along with the distributing state of fillers in the matrix. As a result, further decrease in the size of filler particles to nanoscale (1–100 nm) can lead to the increase in specific surface area between fillers and the polymer and more improvement in the properties of resulting composite [3]. Nowadays, nanomaterial is utilized for improvement in the performance and efficiency of different industrial pieces [4]. Among all used nanofillers in this issue, nanoscale size of clay, silica, and calcium carbonate are the most outstanding improvers of mentioned properties in rubber production industry [5–7].

Nitrile butadiene rubber (NBR) is a polar rubber which has a very high strength against solvents and accordingly, extensive applications in the protection of pipes, automotive, and aviation industries. NBR has a low tensile strength, so adding of fillers to the matrix can help to strengthen its structure. Acrylonitrile content can determine the resistance of rubber against oil materials [7]. Three most frequent methods for the preparation of polymeric nanocomposites are solvent mixing, in situ polymerization, and melt mixing [8].

Although using nanofillers can improve properties of polymer-based matrix, adding of nanoclays alone cannot improve properties of the composite because of the lack of continuity between clay silicate layers and organic polymers. Interaction effect between silicate layers is by the transfer of hydrated cation ion to the organic cation. For instance, octadecyl amine can be enumerated as a surface activator for creation of suitable routes to permeate in the polymeric chain [9]. Organo-clay has lower energy level than the clay and is compatible with the polymer base [7]. Okada and his coworker modified the surface of the clay by the two-stage synthesis. They firstly modified the surface of clay in the form of montmorillonite K 10 and with the use of hydrochloric acid in water and then fabricated clay/NBR nanocomposite by the method of melt mixing and obtained proper mechanical properties and gas permeability [10]. Gureshi et al. added montmorillonite clay fillers to the solid natural rubber by the novel method of two roll mill or modified mill process. They compared process parameters and tensile strength of the fabricated nanocomposite with those of the produced nanocomposites by the method of latex. Results indicated that nanofillers were properly distributed in the polymer and more strengths were observed in the resulting nanocomposite which were prepared by the mill process [9]. In some other works, researchers also investigated the effect of adding nanoclay, organo-clay platelets, modified natural montmorillonite, and organo-modified montmorillonite to reinforce polypropylene–wood flour composites, wood–plastic composites, almond shell flour–polypropylene bio-nanocomposites, and walnut shell/polypropylene composites, respectively [11–14].

Calcium carbonate nanoparticles are a non-organic and inexpensive filler for the preparation of polymer nanocomposites. Nanoscale size of calcium carbonate can improve properties of related nanocomposite depending on its application [15]. Reducing the size of fillers to nanometer scale significantly increased the mechanical and thermal stability of the nanocomposites [16]. Fine distribution of nanofillers in the polymeric matrix will increase strength of the polymer, hardness, and other properties of the nanocomposites [17]. Wu et al. fabricated PVC polymeric nanocomposites filled with calcium carbonate nanoparticles by the method of melt mixing and investigated the mechanical properties, rheology, and morphology of resulting nanocomposites. Their results showed that raising contents of calcium carbonate nanofillers in the polymer matrix caused elongation at breaking point and modulus of elasticity of related nanocomposites to be further improved. Study of rheology properties for produced nanocomposites indicates that increasing amount of calcium carbonate nanofillers will contribute to the melting density of the nanocomposite to be augmented considerably [18]. Nanocomposite of ultrafine vulcanized powdered rubber (UFPR)/poly (vinyl chloride)/calcium carbonate was also fabricated by the endeavor of Wang and his coworkers and properly distribution of non-modified calcium carbonate nanoparticles in the polymer matrix were demonstrated by the TEM imaging [19].

Silica nanoparticles are used in the industry for reinforcement of elastomers as a rheology salt. On the other hand, they can be utilized as the filler in the processing of rubbers and because of their low processing costs and high efficiency, they became more attracted attentions in works of some authors. Li et al. prepared the nanocomposite of nanosilica/nitrile rubber and showed the importance of used nanofiller in the quality improvement in the rubber [20]. Spreading properties of surface non-modified/modified silica nanoparticles with silane group and silica nanoparticles covered with a polymer layer in the matrix of carboxylated nitrile rubber (XNBR) were also studied [21].

The purpose of this investigation is to fabricate NBR-based nanocomposites with high chemical and mechanical stabilities by the application of nanotechnology. Three nanofillers of organo-clay, calcium carbonate, and silica were used to add to the NBR matrix. In situ polymerization method was used for the preparation of nanocomposites. Mechanical and chemical properties of fabricated NBR-based nanocomposites by the addition of nanofillers with the phr content ranging from 1 to 10 were evaluated. Results of rheometric data, FTIR analysis, shore hardness, tensile strength, elongation at break, compression set, and resistance against the ozone and solvent were obtained and discussed for all fabricated nanocomposites. Proposed nanocomposites and their results can be utilized in different applications, such as electronic, automotive, and marine industries, and they can actually be the response for increasingly demand of the industry to multi-functional rubbers.

Experimental

Materials

Polymer as the matrix, nanofillers, agent and vulcanization agent, curing agents, reaction accelerators and anti-oxidation agents are used for synthesize of rubber

composites. These materials were purchased from local markets and are shown in Table 1.

As it can be seen in Table 1, carbon black (with the particle size of 70–96 nm) was also used for the curing of nanocomposites. This material is a conventional filler in this regard for the purpose of improving performances of the nanocomposite and reducing the production costs. Nanoscale materials of clay, calcium carbonate, and silica (fumed) were used in this investigation to add to the NBR matrix. Clay (montmorillonite K 10) and calcium carbonate nanoparticles were purchased from Sigma-Aldrich Chemie GmbH Company (Germany) and the Materials Science Company (USA), respectively. Fumed nanosilica was also purchased from the company of Evonic Industries AG, Germany. The properties of these nanoscale materials are illustrated in Table 2.

Synthesis

Organo-clay

To properly distribute surface particles of clay in the NBR matrix and also intensify the formation of chemical bonds between the clay and NBR, surface modification of the clay was done. For this purpose, octadecylamine was used to create an olephilic (hydrophobic) surface. At first, 20 g of the clay (weighed by an analytical balance with the model of ALJ. 220-4NM, the Kern Company, USA) was distributed in 500 ml of water at 60 °C by the application of a magnetic stirrer (Model D-500, aLFA Company, Iran) to give us clay–water solution. 12.4 g of octadecylamine and 4.6 ml of hydrochloric acid was mixed in 100 ml of water to generate the salt of alkyl ammonium. Obtained solution was poured

Table 1 Used materials for the fabrication of nanocomposites

Materials	Formula	Manufacturer
NBR 6240	Containing 34% of acrylonitrile	Local market
Carbon black (SRF)	–	Local market
Zinc oxide	ZnO	Sigma-Aldrich
Stearic acid	$CH_3(CH_2)_{16}COOH$	Sigma-Aldrich
RD antioxidant (1,2-Dihydro-2,2,4-trimethylquinoline homopolymer)	$C_{12}H_{15}N$	Local market
IPPD antioxidant (N-isopropyl-N′-phenyl-p-phenylenediamine)	$C_{15}H_{18}N_2$	Local market
Plasticizer (dioctyl phthalate)	C_6H_4-1,2-$[CO_2CH_2CH(C_2H_5)(CH_2)_3CH_3]_2$	Sigma-Aldrich
Sulfur	S	Sigma-Aldrich
Accelerator (tetramethylthiuram disulfide)	$(CH_3)_2NCSS_2CSN(CH_3)_2$	Sigma-Aldrich
N-cyclohexyl-2-benzothiazolesulfenamide	$C_{13}H_{16}N_2S_2$	Local market
Octadecyl amine	$(CH_3(CH_2)_{16}CH_2NH_2)$	Sigma-Aldrich
Hydrochloric acid	HCl	Sigma-Aldrich
Distilled water	H_2O	Local market

Table 2 Properties of used nanomaterials (presented by their manufacturers)

Properties	Nanocalcium carbonate	Fumed nanosilica (Aerosil R 200)	Nanoclay
Appearance	White powder	White powder	Pale yellow powder
Average size (nm)	10–45	12 (average size of primary)	1–2
Melting temperature (°C)	825	–	–
Density (g/cm^3)	2.93	2.4	0.5–0.7
Purity (%)	–	99.99	–
Specific surface area (m^2/g)	–	200	220–270

in the clay–water solution and mixed for 1 and 24 h at the ambient temperature and at 60 °C, respectively. The product was then filtered at the room temperature and washed by the distilled water to eliminate the whole silver chloride sediments. Resulting product was dried in the vacuum oven [Model of Vin100, Arta Company, Iran] at 60 °C to obtain organo-clay nanoparticles [22].

Nanocomposites

Rubber contains its common additives and is prepared based on parts per one hundred rubber (phr) and amounts of additives in the rubber based on the phr is the same in all other samples. In this investigation, amounts of used nanoscale additives including nanoorgano-clay, nanocalcium carbonate, and nanosilica were selected to be 1, 3, 5, and 10 phr. Mixing of components was done by the procedure in which nanomaterials were initially mixed by a two roll mill (Brabender, OHG model, Germany) at the mixing condition of the rubber (160 °C) and according to the standard method of ASTM D3187. Other additives of the rubber including carbon black filler, DOP plasticizer, stearic acid, zinc oxide as an activator, anti-oxidizers of IPPD, and RD were also added to the mixture of rubber and nanomaterials by the application of the two roll mill. Amounts of all additives to the rubber are illustrated in Table 3. To investigate the effect of changing nanomaterials contents on the results of nanocomposites, a constant mixing time duration for the production of all samples was used and only variable parameters in the system were the kind and amount of nanomaterials. After 1 day and at the ambient temperature, materials of curing process including the sulfur and accelerators were added to the mentioned mixture by the two roll mill to prevent partial curing of the mixture. Properties of resulted nanocomposites are also dependent on the distribution uniformity of nanoparticles in the polymeric matrix. For instance, distribution of nanoparticles in the NBR matrix has a profound impact on concentrated tension spots and accordingly, an affection on the strength and failure properties of nanocomposites [23]. Witness sample was also produced with the same method and without the presence of nanomaterials.

Table 3 Compositions of fabricated nanomaterial/nitrile rubber nanocomposites

Materials	Mixing condition (Phr)				
	NBR	1 Nano-NBR	3 Nano-NBR	5 Nano-NBR	10 Nano-NBR
NBR	100	100	100	100	100
Nanomaterials	0	1	3	5	10
Carbon black (SRF)	80	80	80	80	80
ZnO	5	5	5	5	5
Stearic acid	1	1	1	1	1
RD	2	2	2	2	2
IPPD	1	1	1	1	1
DOP	10	10	10	10	10
Sulfur	0.5	0.5	0.5	0.5	0.5
TMTD	1	1	1	1	1
CZ	2	2	2	2	2

Cure characteristics of nanocomposites

Curing features of nanocomposites were determined by a rheometer device (model of Gotech, Taiwan) at the temperature of 160 °C and according to the standard method of ASTM D20148. Two important parameters which were obtained from figures of rheometer device are the scorch time (ts_2) and optimum curing time (t_{90}). Scorch time is the time duration in which the amount of torque is increased by 2.26×10^{-2} N m with respect to the minimum amount of the torque. The less the amount of scorch time caused the cross-linking between mixing materials to be increased. Another outstanding parameter is optimum curing time which is the time when we reach to the rate of 90% for the difference between the minimum and maximum amounts of the torque. This parameter can give us a proper evaluation on the amount of curing time for mixtures. The less the amount of optimum curing time, the faster preparation of nanocomposites.

Characterization of nanocomposites

Morphology, size and size distribution of used nanoparticles and their related nanocomposites were analyzed by the Fourier transform infrared spectroscopy (FTIR), scanning electron microscopy (SEM), and transmission electron microscopy (TEM). A spectrometer (model of Perkin Elmer, USA) was used for the FTIR analysis. This technique is based on the absorption of radiation and probing into vibrational jumps of molecules and multi-atomic ions and standard of ISO 4650:2012 was used in this issue [24]. SEM image was recorded by a TESCAN Vega3, Czech Republic.

Mechanical properties

Shore hardness

Hardness of a material is its strength against indentation by a harder material. In the standard hardness tests which have been used in recent years, a hard indenter material will be pressurized to the surface of the sample. As a result, a three-directional tension will be imposed to the pressurized spot. On the other hand, transformation is done in combination with forms of tensile, compressive, and shear. Shore hardness test was done according to the standard method of ASTM D2240. For the test of the rubber, shore A hardness test is used. For determination of the shore A hardness test of nanocomposites, samples with thickness of at least 4 mm are placed on an aligned horizontal hard surface. Shore durometer type of A (code ISH-SAM) will then be rotated to the vertical position somehow that the indenter point has at least 9 mm distance from each edge of the sample. Base of the squeezer, in a way that its surface is parallel to that of the sample, is lifted quickly and without imposing strike. Degree of the indicator device is read after 15 s. This process was repeated for five different spots of the sample with intervals of minimum 6 mm from each other. Averages of obtained values are considered as the shore *A* hardness. Depth of indentation, *D* (mm), which is a criteria for evaluation of the hardness is determined by the following equation [25]:

$$D = 100 - \frac{h}{0.025}$$

where h (mm) is the depth of indentation at the time of imposing the whole force. With this method, the amount of penetration for the indenter to the material is measured in specified conditions.

Tensile strength

This test was conducted based on the standard method of ASTM D412 for dumbbell-shaped test piece. Length of the dumbbell-shaped samples is 20 ± 0.5 mm and the nominal speed of the moving clipper is also 500 mm/min according to the mentioned standard method. All used molds and blades were based on the standard of ISO 4661-1:1993 and molds were also in standard dimensions for preparation of dumbbells. In each point of the thin width mold, deviation from the state of parallel edges should not be larger than 0.05 ml. The device for doing the tensile test should also be in line with the standard condition of ISO 5893:1993. Thickness at the center and two end points of the test piece were measured by the thickness tester and the average measured amounts of surface area were used. In each dumbbell, none of the three measured thin section values should have difference from the average thickness by the amount of more than 2%. Test piece was placed in the tensile test device in a way which lateral and parallel sections at two end points of the test piece were fixed symmetrically and pressure was distributed uniformly on the surface area. The device was turned on and with the nominal velocity of 500 mm/min for the moving

pine, changes in amounts of length and force during experiments were measured with the accuracy of ± 2%. Tensile strength TS (MPa) was determined by:

$$\mathrm{TS} = \frac{F_{\mathrm{m}}}{Wt}$$

where F_{m} (N) is the maximum amount of recorded force, W (mm) is width of the mold thin section, and t (mm) is the thickness of the test piece. Tensile strength at the breaking point ($\mathrm{TS_b}$) was also obtained by this equation:

$$\mathrm{TS_b} = \frac{F_{\mathrm{b}}}{Wt}$$

where F_{b} is the recorded force at breaking point.

Elongation at break

The ability of large deformation of a material is calculated by the parameter of elongation at break. It indicates strength of the whole molecular chains and their movement [26]. Elongation at break (in percentage) of nanocomposites was obtained according to the standard of ASTM D412 and by the following equation [27]:

$$E_{\mathrm{b}} = \frac{100 * \left(L_{\mathrm{b}} - L_0\right)}{L_0}$$

where E_{b} is elongation at break, L_{b} (mm) is length of the test device at breaking point and L_0 (mm) is its initial length, respectively.

Compression set

As the rubber is under pressure, physical and chemical changes can occur in its structure leading to prevention of the rubber to return to its initial dimension after release of the deformation force. Consequently, the amount of compression set for the rubber depends on the time and temperature of the compression and is also dependent on the time and returning temperature. Compression set (C) is determined in the percentage form of the initial compression as follows:

$$C = \frac{h_0 - h_1}{h_0 - h_2} \times 100$$

where h_0 is the initial thickness of the test piece, h_1 is its thickness after returning, and h_2 is the height of spacing. All dimensions are in the scale of millimeter. This test was done in accordance with the standard method of ASTM D395 [28].

Chemical properties

Ozone resistance

In this test, a relative estimation is done on the resistance of the rubber components against weathering in the open space and or in the ozone container (based on the standard of ASTM D2240). For conducting this experiment, rubber piece was placed on the ozone container according to the information mentioned in Table 4. After probing into the rubber piece, if no cracks or fractures were observed on the surface of the sample, the test sample is considered to be resistant against the ozone.

Fluid resistance

To check the resistance of rubbers against liquids or chemical solutions, different solvents are used. According to the literature and different standards, methyl ethyl ketone (MEK) solvent is a proper choice in this regard (It was purchased from Merck Millipur Company). Method of conducting this experiment is in this way that the sample was firstly weighed (W_1) and was then put into the solvent of methyl ethyl ketone at 30 °C. After 48 h, swollen sample was extracted from the solvent and completely dried under the vacuum oven [model of Vin100, Arta Company, Iran] and was weighed again (w_2). The rate of swelling was then calculated from the following equation [22]:

$$\%\text{Swelling} = \frac{w_2 - w_1}{w_1} \times 100$$

Results

Features of nanocomposites curing

Table 5 shows rheometry data of synthesized composites and nanocomposites. For organo-clay/nitrile rubber nanocomposite, the torque generally increases by raising the amount of its contained filler (organo-clay). Its results indicate that adding organo-clay nanoparticles to the NBR matrix will reduce the time duration of cross-linking creation because this polymer is a thermoset containing two components of monomer and hardener. As a result, further increase in the

Table 4 Conditions of conducting test for resistance of the rubber against ozone [ASTM D2240]

Test condition	Amount
Ozone concentration (g/l)	$(50 \pm 5) \times 10^{-8}$
Temperature (°C)	40 ± 2
Time of exposure to ozone (hr)	48
Elongation (%)	20 ± 2
Relative humidity (%)	55 ± 5

percentage rate of admixtures including nanoclay will cause cross-linkings in polymeric chains to be created more conveniently, in smaller intervals, and in lesser time durations than the situation in which nanocomposite contains a specified initial amount of organo-clay nanoparticles. As it was mentioned before, reducing t_{90} will decrease the time duration for the final curing of the product and accordingly, contributes to the process of production for each segment to be faster than that of the final product leading to the increase in production yields.

In nanocalcium carbonate/nitrile rubber nanocomposite, calcium carbonate particles in micron size are generally considered as agglomerated particles which are broken into the initial and smaller particles and distribute in the rubber during the process of curing. Indeed, large particles will cause some problems, such as non-uniform distribution of filler particles, unappropriated appearance, some difficulties in the process, and worse characteristics. This can highlight the essence of homogenization and distribution of particles in the process of curing. Applying nanoscale materials to the nitrile rubber can help particles to distribute properly in the mixture. In addition, organic compounds with low molecular weight including stearic acid can be used in the process of nanocomposite fabrication [29]. According to Table 5, trend of changing the time duration for optimum curing of nanocalcium carbonate/NBR nanocomposites is decreasing. As it can be expected, reducing of t_{90} will decrease final curing of the product and cause the process of production to be faster. This result shows that nanocalcium carbonate particles have isotropic behavior and low nucleation effect and also strong interaction with rubbers, especially NBR polar rubber [30].

Table 5 Rheometry data of studied nanocomposites

	Torque (N m)		Time (min)	
NBR composite	0.46	1.97	1.43	20.10
Organo-clay/NBR nanocomposites				
Phr				
1	0.48	2.01	1.20	18.22
3	0.48	2.25	1.12	17.30
5	0.49	2.34	0.98	17.00
10	0.51	2.46	0.95	16.45
CaCO3/NBR nanocomposite				
1	0.47	2.00	1.31	20.10
3	0.47	2.10	1.22	19.40
5	0.48	2.21	1.14	18.90
10	0.49	2.30	1.00	18.00
SiO2/NBR nanocomposite				
1	0.47	2.05	1.40	20.08
3	0.48	2.28	1.35	20.30
5	0.49	2.36	1.20	20.00
10	0.51	2.72	1.10	19.10

For nanosilica/nitrile rubber nanocomposites, torque is also increased with further raising of the filler particles (nanosilica). Adding 1 phr of nanosilica to the mixture will lead to reduction in the time duration of curing, while time duration of curing is increasing by using other phr content of nanosilica (3, 5, and 10). It should also be mentioned that further raising the amount of nanomaterials can contribute to the decrease of ts_2 indicating the more creation of cross-linkings in the nanocomposite.

Characterization of nanocomposites

Imaging

Figure 1 shows scanning electron microscopy (SEM) image of montmorillonite clay, calcium carnonate and silica nanoparticles. These images reveal the nanoscale size of used particles.

Fourier transform infrared spectroscopy (FTIR)

Figure 2 illustrates the FTIR spectrum for vulcanized NBR rubber without the use of fillers and at the wave range of 4000–400 cm^{-1}. As it can be observed in this figure, molecule indexes of the NBR rubber are characterized in the format of peaks. Peak at the wave number of 2845.30 cm^{-1} is related to the functional group of CH_2 and observed peak at the wave number of 2238.78 cm^{-1} is also regarded to the group of CN and connected bond of C≡N– [31]. The peak at wave numbers of 3521 and 1599.82 cm^{-1} are concerned with the functional group of OH and chemical bond of –C=C–, respectively, in the structure of NBR rubber [32]. According to the standard of rubbers and characterization of acrylonitrile butadiene rubber, the peak at wave numbers of 978.09 cm^{-1} is related to –CH=CH (trans) bond. In fact, carboxylic group and C=O bond both contributed to the formation of a peak at the wave number of 1727.62 cm^{-1} [24].

Figure 3 illustrates the FTIR analysis of used organo-clay nanoparticles and organo-clay/nitrile rubber nanocomposite. In this figure, three major peaks for organo-clay nanoparticles are investigated. At the wave number of 1042.27 cm^{-1}, observed peak is resulted from the absorb specification of –Si–O–Si– in the clay and at the wave number of 1638.16 cm^{-1}, neutral bond of OH caused the creation of another major peak. Then at the wave number of 3621.89 cm^{-1}, the peak for the tensile bond of OH can be observed [33]. In this figure, the FTIR spectrum contains major peaks for both organo-clay and the rubber indicating the proper composite fabrication and creation of appropriate bonds between the two initial materials after curing. In the spectrum of FTIR for organo-clay/NBR nanocomposite at the wave number of 983.86 cm^{-1}, the peak related to the bond of –CH=CH– (trans) in the NBR rubber is observed with a little transition. This transition is due to the addition of organo-clay nanoparticles to the nitrile rubber. The peak at wave number of 1040.56 cm^{-1} is the same as the absorbed major peak of –Si–O–Si– in the organo-clay and this peak will be observed by slightly transition resulted from creation of

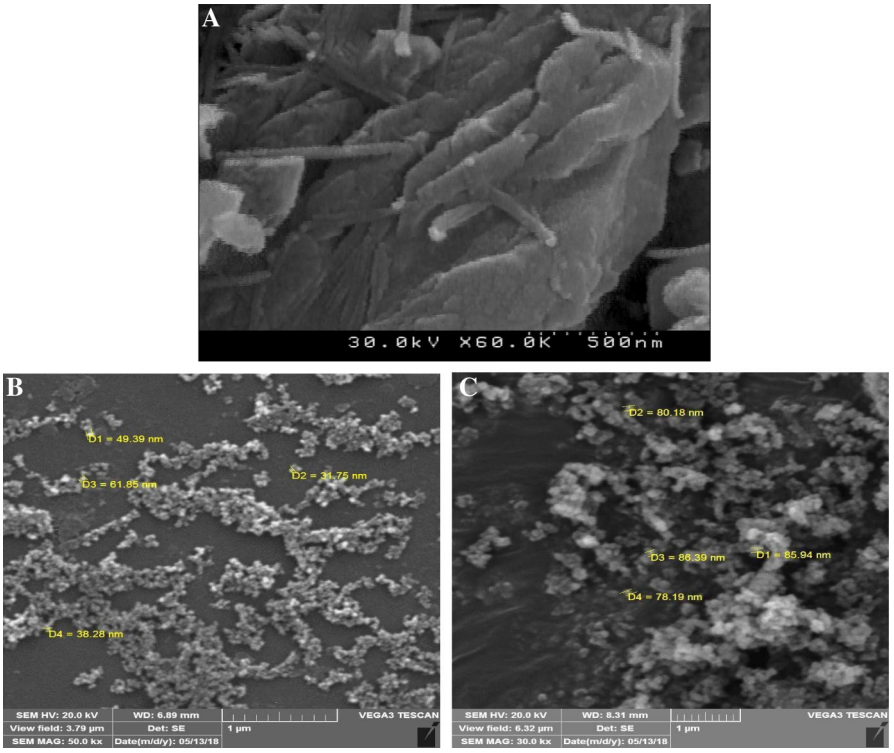

Fig. 1 SEM image for MMT clay, $CaCO_3$, and SiO_2 nanoparticles (from A to C, respectively)

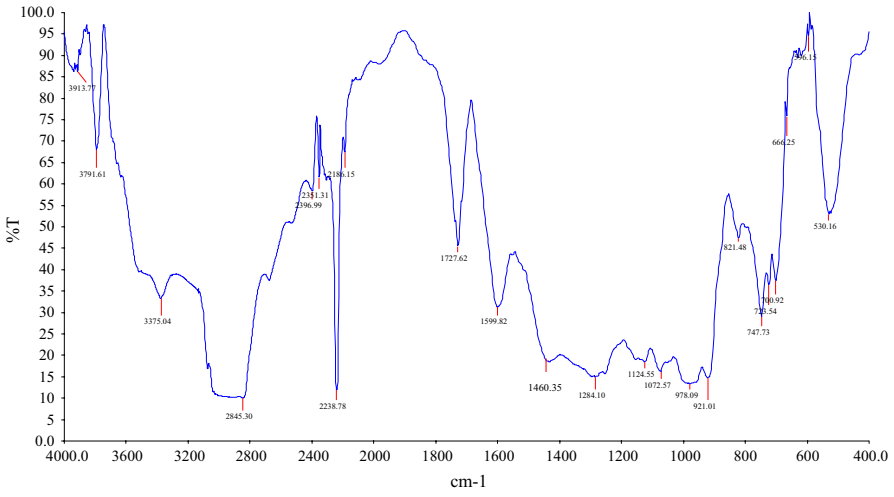

Fig. 2 FTIR spectroscopy of NBR rubber

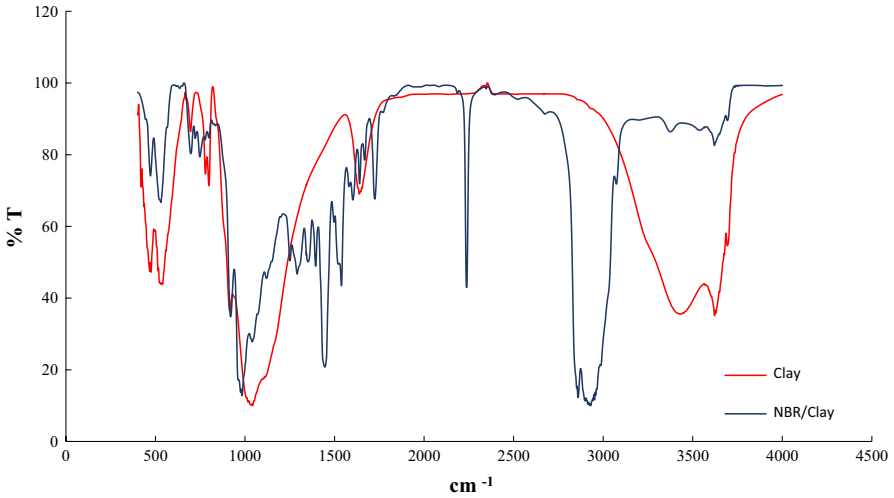

Fig. 3 FTIR spectroscopy of clay nanoparticles and organo-clay/nitrile rubber nanocomposite

polymer-based composite. The peak for the wave number of 2237.25 cm^{-1} is related to the connection bond of –C≡N in the pure NBR rubber. Furthermore, the peak at the wave number of 2930.42 cm^{-1} is due to the presence of CH_2 functional group in the NBR rubber with a little transition to the vulcanized NBR rubber. As a consequence, the obtained peak at wave number of 3620.80 cm^{-1} is resulted from the tensile bond of OH in organo-clay nanoparticles [24, 31, 33].

Figure 4 indicates the results of FTIR spectroscopy for $CaCO_3$ nanoparticles and $CaCO_3$/NBR nanocomposite. According to the mentioned descriptions for Fig. 2 regarding the spectroscopy of vulcanized NBR rubber without the presence of nanoparticles and also Fig. 4, it can be concluded that mixing of calcium carbonate nanoparticles in the rubber after curing was well done. The resulting image from the FTIR spectroscopy of $CaCO_3$ nanoparticles illustrates that peaks at wave numbers of 713.23 and 875.14 cm^{-1}, related to the vibrational bond of carbonate ion in the calcium carbonate, are due to the flexural bond out of the plane and asymmetric tensile in the material, respectively. In addition, wave number of 1414.59 cm^{-1} have three major peaks in the material because of the flexural bond in plane and vibrational bonds of the carbonate ion in calcium carbonate [34]. In this figure, peaks of both the initial materials were determined. Initial peaks regarded to $CaCO_3$ nanoparticles were observed at wave numbers of 713.23, 875.14, and 1414.59 cm^{-1}, respectively. They were seen by a very little transition at wave numbers of 713.02, 875.90, and 1936.99 cm^{-1} in the FTIR spectroscopy of $CaCO_3$/NBR nanocomposite. Peaks at 971.64, 1724.26, 2237.16, and 2851.07 cm^{-1} are related to bonds of –CH=CH–, C=O, C≡N, and CH_2 bonds, respectively, in the structure of NBR [20, 27, 30].

FTIR spectrum of polymer nanocomposites can be used to show the strong bond between the polymer and filler nanoparticles. Analysis of polymer nanocomposites and silica is difficult because of the reflection properties of silica planes. Figure 5 illustrates the results of FTIR spectroscopy for silica nanoparticles and SiO_2/NBR

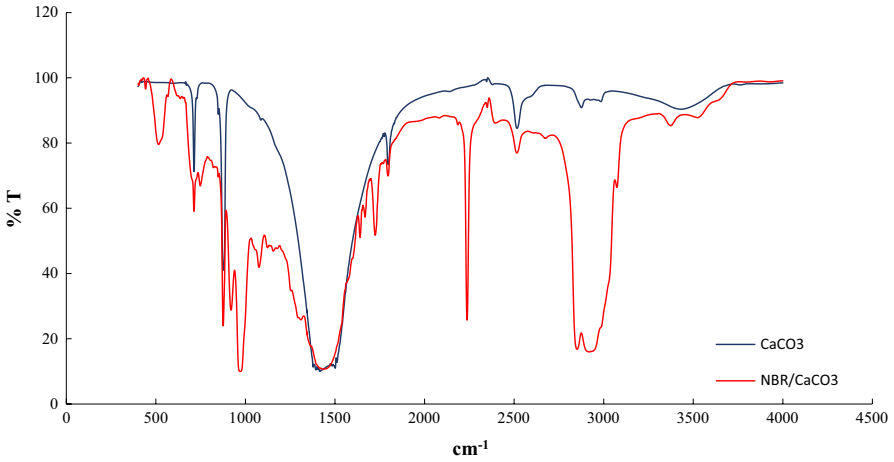

Fig. 4 FTIR spectroscopy for $CaCO_3$ nanoparticles and $CaCO_3$/nitrile rubber nanocomposite

nanocomposite. The major peak of SiO_2 at the wave number of 1103.17 cm^{-1} is regarded to the tensile bond of Si–O observing in the SiO_2/NBR nanocomposite with a transition in the wave number of 1110.95 cm^{-1}. This peak cannot be seen in the spectrum of NBR which does not contain nanosilica [35]. Existing peak at the wave number of 3521 cm^{-1} in Fig. 4 is relevant to the group of OH in the structure of NBR. As silica is added to the NBR, the peak will be transited to the direction of higher bandwidth and wave number of 3433.84 cm^{-1} (Fig. 5). When the connection bond is as –C≡N, wave number of the peak is going to transit from 2238.78 cm^{-1} to 2238.82 cm^{-1} because of the strong bond between –C≡N and SiO_2. In addition, the resulting peak for the bond of –C=C– at the wave number of 1599.82 cm^{-1} will

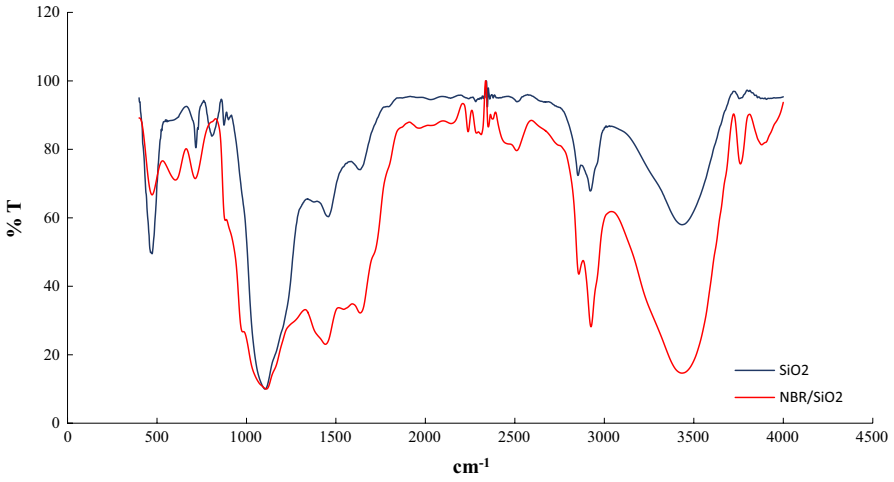

Fig. 5 FTIR spectroscopy for silica nanoparticles and SiO_2/NBR nanocomposite

be transited to 1635.93 cm^{-1} because of the effect for the presence of active surface particles on SiO_2 nanoparticle and NBR [32]. The interesting conclusion is the creation of C–SO_2–N bond at the wave number of 1441.4 cm^{-1} in the SiO_2/NBR nanocomposite. This peak cannot be observed in the spectrum of pure NBR and silica layered. This peak can be created by the reaction of the ammonium salt with zinc–sulfur–amine compound between the silica and NBR during the process of vulcanization [standard of ISO 4650:2012].

All the figures of 2–5 were drew by Microsoft Excel 2013.

Mechanical properties

Figure 6 shows the effect of adding nanofillers in different Phr contents to the NBR matrix on their mechanical properties (drew by OriginPro2016 Software). Shore A hardness, tensile strength, elongation at break, and compression set of the NBR composite and nanocomposites were used to investigate and evaluate their mechanical properties. As it is obvious in this figure, raising the amount of all used nanoparticles leaded to the increase in shore A hardness of their related fabricated nanocomposites. Shore A hardness for the nanocomposite containing 10 phr of organo-clay, calcium carbonate, and silica nanoparticles is 84, 82, and 86, respectively, and has the approximate increase in this property by amounts of 28, 24, and 30%, respectively, with respect to the NBR without the use of nanoparticles.

Two important parameters which are used to determine tensile-stress–strain properties of nanocomposites are tensile strength and elongation at break. In general, tensile strength of composites is directly dependent on their structure and behavior

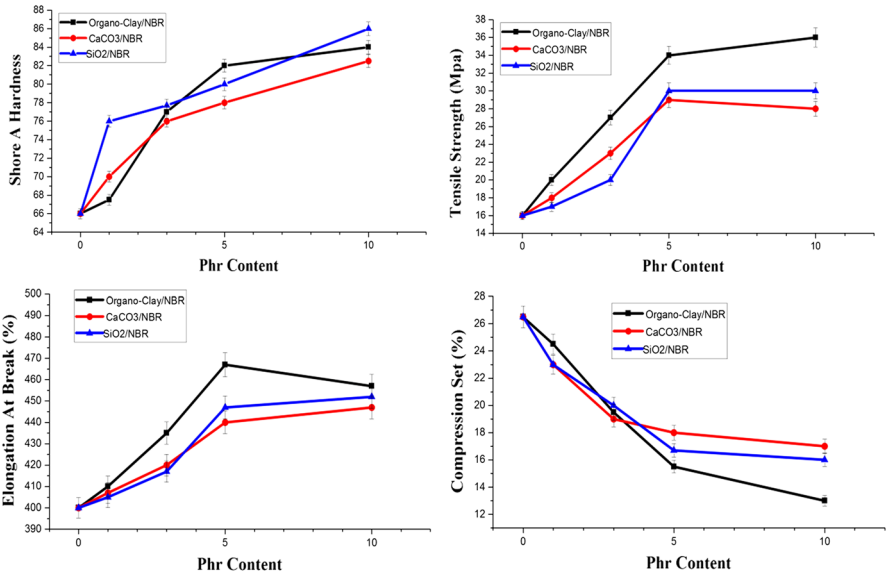

Fig. 6 Mechanical properties of synthesized nanocomposites versus Phr content

of their base matrix. If fillers are distributed properly in the matrix, tensile strength of the resulting composite will also be increased. However, for the case in which distribution of particles in the polymer matrix is asymmetric, tensile strength of the composite will be reduced because of the formation of concentrated tension points in the matrix. This behavior is obvious in fillers with micron sizes [23]. Nanoscale structures in the same weight percentages as for the particles with micron sizes can tackle mentioned problem because of better distribution of nanoparticles in the matrix and also their smaller sizes. It should also be noted that less increase in weight percentages of materials in nanoscale can improve different properties of the composite with respect to materials in micron scale [7, 30].

It can be detected from Fig. 6 that nanocomposite containing 10 phr of organo-clay nanoparticles has the maximum amount of tensile strength with respect to that of other fabricated nanocomposites. In addition, organo-clay/NBR nanocomposite devoted the highest amount of tensile strength in the whole studied phr contents of nanoadditives with respect to that of other prepared nanocomposites. Raising the amount of calcium carbonate nanoparticles to the amount of 5 phr caused the tensile strength of related nanocomposite to be increased, while the use of 10 phr of calcium carbonate nanoparticle in mentioned nanocomposite leaded its tensile strength to be reduced in comparison with the use of 5 phr nanoparticle in NBR matrix. On the other hand, 5 phr of $CaCO_3$ is the optimum amount of nanoadditives to be applied to $CaCO_3$/NBR nanocomposite. For SiO_2/NBR nanocomposite, raising the amount of nanosilica to 5 phr caused its tensile strength to be increased, while further raising the amount of nanosilica in this nanocomposite contributed to no change in tensile strength of related nanocomposite.

It is also clear in this Fig. 6 that raising the amount of nanomaterials as fillers in the nitrile rubber matrix increased the elongation at break percentages of synthesized nanocomposites, while for the case in which raising of the organo-clay nanoparticles content from 5 to 10 phr caused the elongation at break of related nanocomposite to be reduced. Elongation at break percentages for the NBR and organo-clay/NBR nanocomposite with 5 phr of their nanoadditive were 400 and 467, respectively, while percentage of elongation at break for Nano-$CaCO_3$/NBR and Nano-SiO_2/NBR nanocomposites with 10 phr content of nanoadditives were found to be 448 and 452, respectively. This figure also indicate that adding 1 and 3 phr of nanoadditives to Nano-$CaCO_3$/NBR nanocomposite caused its elongation at break percentage to be more than that of Nano-SiO_2/NBR nanocomposite with the same content of nanoadditives. However, results of elongation at break percentage for the use of 5 and 10 phr of nanoadditives in Nano-$CaCO_3$/NBR nanocomposite showed to be lower than that of Nano-SiO_2/NBR nanocomposite with the same phr content of nanoadditives.

Experiments for measurement of compression set percentage of samples were conducted at 100 °C and for the time duration of 72 h. Results indicate that adding nanoadditives to the samples will reduce their deformation resulting from impose of the pressure force to structure of nanocomposites. Compression set for 3, 5, and 10 phr of $CaCO_3$/nitrile rubber nanocomposites were slightly reduced. As a result, phr of 3 can be considered as the optimum amount of calcium carbonate nanoparticle in the related nanocomposite. For SiO_2/nitrile rubber nanocomposite,

compression set was reduced from 26.5 to 15.8% by adding 10 phr of nanosilica to the related composite. Comparing results for the compression set of studies nanocomposites indicates that adding 1 phr of nanoadditives to the composites caused organo-clay/NBR nanocomposite to have the highest amount of compression set among that of other two nanocomposites, while adding 3 phr of nanoadditive to SiO2/NBR nanocomposite leaded its compression set to has the largest value than that of other two ones. However, for the case in which 5 and 10 phr of nanoadditive are added to composites, compression set for CaCO3/NBR nanocomposite obtained the highest amounts with respect to that of other synthesized nanocomposites.

Chemical properties

Ozone resistance

Results indicate that all produced samples including pristine nitrile rubber and nanocomposites are resistant against the ozone because no crack was observed on the surface of samples during the time of conducting this test and at its specified condition.

Resistance in methyl ethyl ketone (MEK) solvent

Table 6 shows the swelling rate of produced nanocomposites in MEK solvent. Non-vulcanized NBR was completely solved in the MEK solvent, while vulcanized NBR did not solve in this solvent and their rate of swelling is dependent on their cross-linkings and nanoadditives. This table indicates that organo-clay/NBR nanocomposite has better barrier properties than the vulcanized NBR. With respect to the information available in the literature [36, 37], Table 6, and Fig. 7, NBR nanocomposites containing organo-clay nanoparticles caused the swelling rate of final product to be reduced and accordingly, increased their resistance against the MEK solvent. However, this reduction in the swelling rate for other two fabricated nanocomposites found to be less than that of organo-clay/NBR nanocomposite by further raising of the phr for nanoadditives in their structures.

Conclusions

Elastomeric nanocomposites containing nitrile rubber and nanofillers of nanoorgano-clay, nanocalcium carbonate, and nanosilica with different phr contents (1, 3, 5, and 10) were synthesized properly. The interaction between nanofillers and NBR-based matrix were determined by the analysis of FTIR. According to the results of rheometry and curing conditions for nanocomposites, organo-clay/nitrile rubber nanocomposite with 10 phr of organo-clay nanoparticles had the best curing conditions by the time duration of 16.45 min indicating the reduction of curing time by the rate of 18% and also increase in the rate of nanocomposite production. Obtained results also showed that the shore hardness for all studied nanocomposites

Table 6 Swelling rate of studied nanocomposites in MEK solvent

Sample tests	Swelling in MEK solvent (%)
Non-vulcanized NBR	Will be solved
Vulcanized NBR	165
Organo-clay/NBR nanocomposites	
Phr	
1	158
3	140
5	130
10	115
CaCO3/NBR nanocomposite	
1	163
3	153
5	145
10	142
SiO2/NBR nanocomposite	
1	164
3	155
5	148
10	137

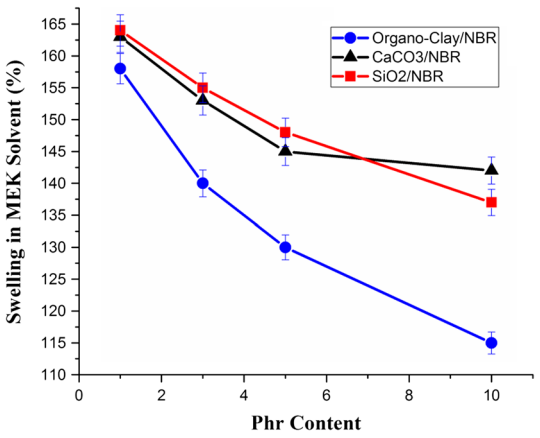

Fig. 7 Chemical properties of synthesized nanocomposites versus Phr content

were increased by further raising of their nanofillers phr contents. In this regard, the nanocomposite with phr content of 10 for nanosilica devoted the highest amount of shore hardness than that of other nanocomposites and caused its shore hardness to be increased by the rate of 30.3% with respect to the nitrile-based rubber without the usage of nanofillers. Investigation on the tension stress–strain properties of used nanocomposites were conducted by probing into two parameters of tensile strength and elongation at breaking point of them with changing the phr content of

nanofillers. Highest tensile strength rate was obtained for the nitrile rubber containing 10 phr of organo-clay by the amount of 36 MPa and the increase rate of 125% with respect to the nitrile rubber. Additionally, nitrile rubber nanocomposite tailored by 5 phr of organo-clay caused the elongation at breaking point to be increased by 467% and accordingly, it had the best performance among all other fabricated nanocomposites in this regards. Nitrile rubber nanocomposite endowed with 10 phr of organo-clay nanoparticles had the lowest rate of compression set (deformation by imposing pressure) than that of other studied nanocomposites. Compression set of 13.2% was obtained for the mentioned nanocomposite. Resistance of fabricated nanocomposites against the solvent was determined by measuring their swelling rate in methyl ethyl ketone solvent. Their results showed that organo-clay (10 phr)/nitrile rubber nanocomposite devoted the lowest amount of swelling rate in the solvent by 115% with respect to that of other used nanocomposites. According to the very low costs of purchasing for clay nanoparticles and parameters of accessibility and improved properties of nanocomposites, it was concluded that nitrile rubber nanocomposite containing 10 phr of organo-clay is the best choice than other ones to be chosen as an improved nanocomposite in different industrial applications. It should also be noted that further increase in the stability of clay nanoparticles in the NBR matrix can be attained by using of octadecylamine, as a surface activator.

Acknowledgements Authors are grateful to the Fars Science & Technology Park for preparing equipped laboratories for conducting tests in the manuscript and extend their appreciations to MS Fatemeh Sadeghzadeh.

Compliance with ethical standards

Conflict of Interest The authors declare that they have no conflict of interest.

References

1. Cao X, Xu C, Wang Y et al (2013) New nanocomposite materials reinforced with cellulose nanocrystals in nitrile rubber. Polym Test 32:819–826. https://doi.org/10.1016/j.polymertesting.2013.04.005
2. Sadeghalvaad M, Sabbaghi S (2015) The effect of the TiO_2/polyacrylamide nanocomposite on water-based drilling fluid properties. Powder Technol 272:113–119. https://doi.org/10.1016/j.powtec.2014.11.032
3. Sengupta R, Chakraborty S, Bandyopadhyay S et al (2007) A short review on rubber/clay nanocomposites with emphasis on mechanical properties. Polym Eng Sci 47:1956–1974. https://doi.org/10.1002/pen.20921
4. Asmatulu R, Nguyen P, Asmatulu E (2013) Nanotechnology safety in the automotive industry. In: Asmatulu R (ed) Nanotechnology safety, chap 5. Elsevier, Amsterdam, pp 57–72. ISBN 9780444594389. https://doi.org/10.1016/B978-0-444-59438-9.00005-9
5. Senthivel K, Manikandan K, Prabu B (2015) Studies on the mechanical properties of carbon black/halloysite nanotube hybrid fillers in nitrile rubber nanocomposites. Mater Today Proc 2:3627–3637. https://doi.org/10.1016/j.matpr.2015.07.118
6. Satyanarayana MS, Bhowmick AK, Dinesh Kumar K (2016) Preferentially fixing nanoclays in the phases of incompatible carboxylated nitrile rubber (XNBR)-natural rubber (NR) blend using thermodynamic approach and its effect on physico mechanical properties. Polymer (Guildf) 99:21–43. https://doi.org/10.1016/j.polymer.2016.06.063

7. Eyssa HM, Abulyazied DE, Abdulrahman M, Youssef HA (2017) Mechanical and physical properties of nanosilica/nitrile butadiene rubber composites cured by gamma irradiation. Egypt J Pet. https://doi.org/10.1016/j.ejpe.2017.06.004
8. Luan J, Wang S, Hu Z, Zhang L (2012) Synthesis techniques, properties and applications of polymer nanocomposites. Curr Org Synth 9:114–136. https://doi.org/10.2174/157017912798889161
9. Qureshi MN, Qammar H (2010) Mill processing and properties of rubber–clay nanocomposites. Mater Sci Eng, C 30:590–596. https://doi.org/10.1016/j.msec.2010.02.008
10. Okada A, Usuki A (1995) The chemistry of polymer-clay hybrids. Mater Sci Eng, C 3:109–115. https://doi.org/10.1016/0928-4931(95)00110-7
11. Khanjanzadeh H, Tabarsa T, Shakeri A (2012) Morphology, dimensional stability and mechanical properties of polypropylene–wood flour composites with and without nanoclay. J Reinf Plast Compos 31:341–350. https://doi.org/10.1177/0731684412438793
12. Khanjanzadeh H, Tabarsa T, Shakeri A, Omidvar A (2011) Effect of organoclay platelets on the mechanical properties of wood–plastic composites formulated with virgin and recycled polypropylene. Wood Mater Sci Eng 6:207–212. https://doi.org/10.1080/17480272.2011.606915
13. Zahedi M, Khanjanzadeh H, Pirayesh H, Saadatnia MA (2015) Utilization of natural montmorillonite modified with dimethyl, dehydrogenated tallow quaternary ammonium salt as reinforcement in almond shell flour–polypropylene bio-nanocomposites. Compos B Eng 71:143–151. https://doi.org/10.1016/j.compositesb.2014.11.009
14. Zahedi M, Pirayesh H, Khanjanzadeh H, Tabar MM (2013) Organo-modified montmorillonite reinforced walnut shell/polypropylene composites. Mater Des 51:803–809. https://doi.org/10.1016/j.matdes.2013.05.007
15. Sahebian S, Zebarjad SM, Khaki JV, Sajjadi SA (2009) The effect of nano-sized calcium carbonate on thermodynamic parameters of HDPE. J Mater Process Technol 209:1310–1317. https://doi.org/10.1016/j.jmatprotec.2008.03.066
16. Zebarjad SM, Sajjadi SA (2008) On the strain rate sensitivity of HDPE/$CaCO_3$ nanocomposites. Mater Sci Eng, A 475:365–367. https://doi.org/10.1016/j.msea.2007.05.008
17. Wang Q, Song Q, Qiao J et al (2011) Good dispersion of hydrophilic nanoscale calcium carbonate particles in nitrile butadiene rubber matrix. Polymer (Guildf) 52:3496–3502. https://doi.org/10.1016/j.polymer.2011.05.037
18. Wu D, Wang X, Song Y, Jin R (2004) Nanocomposites of poly(vinyl chloride) and nanometric calcium carbonate particles: effects of chlorinated polyethylene on mechanical properties, morphology, and rheology. J Appl Polym Sci 92:2714–2723. https://doi.org/10.1002/app.20295
19. Wang Q, Zhang X, Dong W et al (2007) Novel rigid poly(vinyl chloride) ternary nanocomposites containing ultrafine full-vulcanized powdered rubber and untreated nano-sized calcium carbonate. Mater Lett 61:1174–1177. https://doi.org/10.1016/j.matlet.2006.06.078
20. Li J, You L, Tang S-K (2014) A process to prepare high-quality natural rubber silica masterbatch by liquid phase mixing, Patent Application WO2016014037A1, issued: 2016-01-28
21. Sala RL, Arantes TM, Longo E et al (2014) Evaluation of modified silica nanoparticles in carboxylated nitrile rubber nanocomposites. Colloids Surf A Physicochem Eng Asp 462:45–51. https://doi.org/10.1016/j.colsurfa.2014.08.012
22. Kim J, Oh T, Lee D (2003) Morphology and rheological properties of nanocomposites based on nitrile rubber and organophilic layered silicates. Polym Int 52:1203–1208. https://doi.org/10.1002/pi.1249
23. Taguet A, Cassagnau P, Lopez-Cuesta J-M (2014) Structuration, selective dispersion and compatibilizing effect of (nano)fillers in polymer blends. Prog Polym Sci 39:1526–1563. https://doi.org/10.1016/j.progpolymsci.2014.04.002
24. da Silva ALN, Rocha MCG, Moraes MAR et al (2002) Mechanical and rheological properties of composites based on polyolefin and mineral additives. Polym Test 21:57–60. https://doi.org/10.1016/S0142-9418(01)00047-2
25. Ishida H (1988) Interfaces in polymer, ceramic, and metal matrix composites. In: Proceedings of the second international conference on composite interfaces (ICCI-II), Cleveland, OH, June 13–17, 1988
26. Liu Yingbin, Na Li MR (2013) Toughening poly (trimethylene terephthalate) by maleinized acrylonitrile–butadiene–styrene. Macromol Indian J 9:91–101
27. Li Y, Wu X, Song J et al (2017) Reparation of recycled acrylonitrile–butadiene–styrene by pyromellitic dianhydride: reparation performance evaluation and property analysis. Polymer (Guildf) 124:41–47. https://doi.org/10.1016/j.polymer.2017.07.042

28. Kohjiya S, Ikeda Y (2000) Reinforcement of general-purpose grade rubbers by silica generated in situ. Rubber Chem Technol 73:534–550. https://doi.org/10.5254/1.3547604
29. Poh BT, Kwok CP, Lim GH (1995) Reversion behaviour of epoxidized natural rubber. Eur Polym J 31:223–226. https://doi.org/10.1016/0014-3057(94)00167-7
30. Poh BT, Ismail H, Tan KS (2002) Effect of filler loading on tensile and tear properties of SMR L/ENR 25 and SMR L/SBR blends cured via a semi-efficient vulcanization system. Polym Test 21:801–806. https://doi.org/10.1016/S0142-9418(02)00014-4
31. Zuiderduin WC, Westzaan C, Huétink J, Gaymans R (2003) Toughening of polypropylene with calcium carbonate particles. Polymer (Guildf) 44:261–275. https://doi.org/10.1016/S0032-3861(02)00769-3
32. Poh BT, Ismail H, Quah EH, Chin PL (2001) Cure and mechanical properties of filled SMR L/ENR 25 and SMR L/SBR blends. J Appl Polym Sci 81:47–52. https://doi.org/10.1002/app.1411
33. Preetha Nair K, Thomas P, Joseph R (2012) Latex stage blending of multiwalled carbon nanotube in carboxylated acrylonitrile butadiene rubber: mechanical and electrical properties. Mater Des 41:23–30. https://doi.org/10.1016/j.matdes.2012.04.021
34. Hanas VK, Hanas T (2016) Development and characterization of NBR/silica nanocomposites. J Mater Sci Mech Eng 3:27–30
35. Hwang W-G, Wei K-H, Wu C-M (2004) Mechanical, thermal, and barrier properties of NBR/organosilicate nanocomposites. Polym Eng Sci 44:2117–2124. https://doi.org/10.1002/pen.20217
36. Al-Hosney HA, Grassian VH (2005) Water, sulfur dioxide and nitric acid adsorption on calcium carbonate: a transmission and ATR-FTIR study. Phys Chem Chem Phys 7:1266. https://doi.org/10.1039/b417872f
37. Rajkumar K, Ranjan P, Thavamani P, Jeyanthi P, Pazhanisamy P (2013) Dispersion studies of nanosilica in NBR based polymer nanocomposite. Rasayan J Chem 6:122–133